https://doi.org/10.5194/acp-2020-1070
Preprint. Discussion started: 8 December 2020

Atmospheric Chemistry and Physics Discussions

On the similarities and differences between the products of oxidation of hydrocarbons under simulated atmospheric conditions and cool-flames.

Roland Benoit [1] Nesrine Belhadj[1,2], Maxence Lailliau[1,2], and Philippe Dagaut[1]

[1]CNRS-INSIS, ICARE, Orléans, France, roland.benoit@cnrs-orleans.fr, nesrine.belhadj@cnrs-orleans.fr, maxence.lailliau@cnrs-orleans.fr, dagaut@cnrs-orleans.fr
[2]Université d'Orléans, Orléans, France

Correspondence: Benoit Roland (roland.benoit@cnrs-orleans.fr)

Abstract. Whereas the kinetics of oxidation of limonene has been extensively studied and mechanisms for its oxidation by OH and/or ozone have been proposed, more studies are required for better understanding its oxidation pathways. The oxidation of limonene-oxygen-nitrogen mixtures was studied using a jet-stirred reactor at elevated temperature and atmospheric pressure. Samples of the reacting mixtures were collected and analyzed by high resolution mass spectrometry (Orbitrap) after direct injection or after separation by reverse-phase ultra-high-pressure liquid chromatography and soft ionization by (+/-) HESI and (+/-) APCI. The results indicate that among the 1138 detected products, many oxygenates found in earlier studies of limonene oxidation by OH and/or ozone are also produced under the present conditions. Other highly oxygenated products and oligomers were also detected in the present work. The results are discussed in terms of reaction pathways involving the initial formation of peroxy radicals, isomerization reactions yielding keto-hydroperoxides and other oxygenated intermediates and products up to $C_{25}H_{32}O_{17}$. The possible occurrence of the Waddington mechanism and of the Korcek mechanism are also discussed. The present work demonstrates similarities between the oxidation products and oxidation pathways of limonene under simulated atmospheric conditions and in those encountered during the self-ignition of hydrocarbons at low temperatures, which should stimulate future interactions between communities of atmospheric chemistry and combustion chemistry to improve current chemical models.

1. Introduction

Terpenes are emitted by vegetation; they represent a large fraction of the volatile organic compounds (VOCs) present in the troposphere (Seinfeld and Pandis, 2006;Llusia` and Penuelas, 2000). These cyclic hydrocarbons are also considered as potential high-density biojet fuels (Pourbafrani et al., 2010;Meylemans et al., 2012;Harvey et al., 2010;Harvey et al., 2015). Their use as drop-in ground transportation fuel could also be of interest, considering their cetane number around 20 (Yanowitz

https://doi.org/10.5194/acp-2020-1070
Preprint. Discussion started: 8 December 2020

Atmospheric Chemistry and Physics Discussions

et al., 2017). The atmospheric oxidation kinetics of terpenes has been extensively studied, although we are far from a detailed understanding of the many processes involved (Berndt et al., 2015).

α-Pinene, β-pinene, and limonene are among the most abundant terpenes in the troposphere (Witkowski and Gierczak, 2017;Zhang et al., 2018). Their oxidation can yield a large variety of oxygenated organic compounds such as highly oxygenated molecules (HOMs) which are considered to play an important role in secondary organic aerosols (SOA) formation (Bianchi et al., 2019).

Recently, Kourtchev et al. have shown that the concentration of SOA (directly related to that of VOC) mainly influences the apparition of oligomers whereas environmental or experimental conditions (RH, ozonolysis vs. OH-oxidation/photolysis, long-term atmospheric aging) preferentially influences the evolution of these oligomers (Kourtchev et al., 2016). This initial concentration is presented as one of the determining factors of the chemical nature of SOAs and their evolution into oligomers. The so-called cool flame combustion makes it possible to study the formation of SOA and oligomers under conditions of high VOC concentration and elevated temperature (T=520K here). Moreover, the absence of ozone, and no need for the addition of a scavenger, allows probing reaction mechanisms and observing chemical species potentially specific to this mode of oxidation. In combustion (Benson, 1981;Cox and Cole, 1985;Morley, 1987), it is commonly accepted that the low-temperature oxidation of hydrocarbons (RH), also named cool-flame, can lead to the formation of oxygenated intermediates, but generally, it is assumed that the auto-oxidation proceeds through the formation of keto-hydroperoxides (KHPs) which provide chain branching by decomposition: RH + OH ⇆ R + H_2O, R+ O_2 ⇆ ROO, ROO ⇆ QOOH, QOOH + O_2 ⇆ OOQOOH, OOQOOH ⇆ HOOQ'OOH ⇆ HOOQ'O + OH, HOOQ'O ⇆ OQ'O + OH. However, recent studies reported the formation of HOMs during the so-called low-temperature oxidation (500–600 K) of hydrocarbons and other organics (alcohols, aldehydes, ethers, esters) (Wang et al., 2018;Wang et al., 2017b;Belhadj et al., 2020). There, the H-atom transfer in the OOQOOH intermediate does not involve the H-C-OOH group but another H-C group, opening new oxidation pathways. Such alternative pathways do not yield ketohydroperoxides, and a third O_2 addition to HOOQ'OOH yielding OOQ'$(OOH)_2$ can occur. This sequence of reactions can proceed again, yielding highly oxygenated products (Wang et al., 2017b;Belhadj et al., 2020;Belhadj et al., 2021). Also, QOOH can decompose via: QOOH → OH + cyclic ether, QOOH → OH + carbonyl + olefin, and QOOH → HO_2 + olefin. In few studies devoted to the understanding of atmospheric oxidation mechanism of hydrocarbons yielding highly oxidized products, auto-oxidation was proposed as a pathway to organic aerosols, e.g. (Jokinen et al., 2014a;Jokinen et al., 2015;Mutzel et al., 2015;Berndt et al., 2016;Crounse et al., 2013;Ehn et al., 2014). The early H-shift, ROO ⇆ QOOH, is favored by increased temperature, which explains its importance in autoignition, but the presence of substituents such as OH, C=O, and C=C in the ROO radical can significantly increase the rate of H-shift making it of significance at atmospheric temperatures (Bianchi et al., 2019).

Besides these processes, the Waddington mechanism (Ray et al., 1973), involving OH and O_2 successive additions on a C=C double bond, followed by H-atom transfer from –OH to –OO, can occur, yielding carbonyl compounds: R-C=C-R' + OH ⇆ R-C-C(-R')-OH, R-C-C(-R')-OH + O_2 ⇆ OO-C(-R)-C(-R')-OH ⇆ HOO-C(-R)-C(R')-O ⇆ OH + R-C=O + R'-C=O. The

https://doi.org/10.5194/acp-2020-1070
Preprint. Discussion started: 8 December 2020


Atmospheric Chemistry and Physics Discussions

Korcek mechanism(Jensen et al., 1981) through which γ-ketohydroperoxides are transformed into a carboxylic acid and a carbonyl compound can occur too. The formation of carboxylic acids and carbonyl products via the Korcek mechanism has already been postulated by Mutzel et al. (Mutzel et al., 2015) whereas it is frequently considered in recent kinetic combustion modeling (Ranzi et al., 2015).

Then, questions arise: what are the similarities and differences between the products of oxidation of hydrocarbons under simulated atmospheric conditions and cool-flames? Do oxidation routes observed in auto-oxidation (cool flames) play a significant role under atmospheric conditions?

This work aims at characterizing the oxidation products of limonene, which has higher tendency to form HOMs by simulated atmospheric oxidation than more abundant monoterpenes (e.g., α-pinene and β-pinene) (Jokinen et al., 2015) and compare the results with literature data obtained under atmospheric oxidation. To this end, we studied the oxidation of limonene-oxygen-nitrogen mixtures in a jet-stirred reactor (JSR) at atmospheric pressure, large excess of oxygen, and elevated temperature. Our results are compared to literature data obtained under tropospheric relevant conditions where terpenes are oxidized by OH and/or ozone. For sake of clarity, the present oxidation experiments will be called “auto-oxidation” in the following sections.

2. Experiments

The present experiments were carried out in a fused silica jet-stirred reactor (JSR) setup presented earlier (Dagaut et al., 1986) and used in previous studies (Dayma et al., 2011;Dagaut and Lecomte, 2003;Dagaut et al., 1998). As in earlier works (Thion et al., 2017;Dayma et al., 2011) limonene (R)-(+) (>97% pure from Sigma-Aldrich) was pumped by an HPLC pump (Shimadzu LC10 AD VP) with an online degasser (Shimadzu DGU-20 A3) and sent to a vaporizer assembly where it was diluted by a nitrogen flow. Limonene and oxygen were sent separately to a 42 mL JSR to avoid oxidation before reaching the injectors (4 nozzles of 1 mm I.D.) providing stirring. The flow rates of nitrogen and oxygen were controlled by mass flow meters. Good thermal homogeneity along the vertical axis of the JSR was recorded (gradients of < 1 K/cm) by thermocouple measurements (0.1 mm Pt-Pt/Rh-10% wires located inside a thin-wall silica tube). The oxidation of 1% limonene ($C_{10}H_{16}$) under fuel lean conditions (equivalence ratio of 0.25, 56 %O_2, 43 %N_2) was studied at 590 K, atmospheric pressure, and at a residence time of 2 s. A low-pressure sonic probe was used to freeze the reactions and take samples. To measure low-temperature oxidation products ranging from hydroperoxides, ketohydroperoxides (KHPs), to highly oxidized molecules, the sonic probe samples were bubbled into cooled acetonitrile (UHPLC grade ≥99.9, T= 0°C, 250 mL) for 90 min. The resulting solution was stored in a freezer at -30°C. Analyses were performed by direct sample instillation (FIA- HESI/APCI settings sheath gas 12 a.u. auxiliary gas flow 0, capillary temperature 120°C, spray voltage 3.8 kV, flow injection of 3µL/min recorded for 1 min for data averaging) in the ionization chamber of a high resolution mass spectrometer (Orbitrap® Q-Exactive from Thermo Scientific, mass resolution of 140,000 and mass accuracy <0.5 ppm RMS). Mass calibrations in positive and negative HESI were performed using Pierce™ calibration mixtures (Thermo Scientific). Ultra-high pressure liquid chromatography (UHPLC) analyses were performed using an analytical column at a controlled temperature of 40°C (C_{18} Phenomenex Luna, 1.6µm, 100 Å, 100x2.1

https://doi.org/10.5194/acp-2020-1070
Preprint. Discussion started: 8 December 2020

Atmospheric Chemistry and Physics Discussions

mm) for products separation after injection of 3 µL of sample eluted by water-acetonitrile (ACN) at a flow rate of 250 µL/min (gradient 5% to 90% CAN, during 14 min). Both heated electrospray ionization (HESI) and atmospheric chemical ionization (APCI) were used in positive and negative modes for the ionization of products. APCI settings were: vaporizer temperature of 120°C, sheath gas flow of 55 a.u., auxiliary gas flow of 6 a.u., sweep gas flow of 0 a.u., capillary temperature of 300°C, corona current of 3µA. In HESI mode, we used a spray voltage of 3.8 kV. Because oxidation of analytes in HESI has been reported previously (Pasilis et al., 2008;Chen and Cook, 2007), we verified that no significant oxidation occurred in the HESI and APCI ion sources by injecting a limonene-ACN mixture. HESI source is suitable for the detection of high masses, but also HOMS and the presence of salt adducts remains insignificant (Kourtchev et al., 2020). To determine the structure of limonene oxidation products, MS-MS analyses were performed at collision cell energy of 10–30 eV. 2,4-Dinitrophenylhydrazine (DNPH) was also used to characterize carbonyl compounds. As in previous work (Wang et al., 2017b;Belhadj et al., 2020), the fast OH/OD exchange was used to prove the presence of hydroxyl or hydroperoxyl functional groups in the products. We added 300 µL of D_2O (Sigma-Aldrich) to 1.5 mL of sample. The resulting solution was analyzed by flow injection and HESI/APCI mass spectrometry.

3. Data Processing

High-resolution mass spectrometry (HR-MS) generates a significant amount of data that is easier to interpret with two- or three-dimensional visualization tools (Nozière et al., 2015;Wang et al., 2017a;Walser et al., 2008;Tu et al., 2016). In this study, we used Kendrick's mass analysis, double bond equivalent (DBE), van Krevelen diagrams, and carbon oxidation state (OS_c). Kendrick's mass analysis (Sleno, 2012;Hughey et al., 2001;Kune et al., 2019) allows representing in two dimensions and in a new reference frame, a complex mass spectrum of an organic mixture. This reference frame is based on a mass defect calculated from structural units (CH_2, O, CHO, ...). In a Kendrick representation, the homologous series (constructed by the repeated addition of structural units CH_2, O, CHO, ...) are aligned on the same horizontal line. This mass defect is calculated by the difference between the Kendrick mass and the nominal mass. In this study, CH_2 was chosen as the structural unit.

In Kendrick's plots, the X-axis represents the Kendrick Mass

$$(\boldsymbol{CH_2}) = \boldsymbol{observed\ mass} * \frac{\boldsymbol{nominal\ mass\ of\ CH_2}}{\boldsymbol{exact\ mass\ of\ CH_2}},$$

and the Y-axis represents the Kendrick Mass Defect

$$(\boldsymbol{CH_2}) = \boldsymbol{nominal\ mass} - \boldsymbol{Kendrick\ mass}\ (\boldsymbol{CH_2})$$

The belonging of unknown chemical compounds to an homogeneous series of compounds can be used for their identification. The number of double bond equivalent (DBE) represents the sum of the number of unsaturation and ring present in a compound (Nozière et al., 2015). The decrease in the number of hydrogen atoms increases its value, but it is independent of the number

https://doi.org/10.5194/acp-2020-1070
Preprint. Discussion started: 8 December 2020

Atmospheric Chemistry and Physics Discussions

of oxygen atoms. It can be used to identify certain groups of chemical compounds or reaction mechanisms (Kundu et al., 2012). The decimal values of this number were not taken into account in this study. The van Krevelen diagram (Kim et al., 2003;Van Krevelen, 1950) shows the evolution of the H/C ratio as a function of O/C for a set of identified molecules. In a complex organic mixture, it allows classifying the chemical products according to their degree of oxidation or their degree of reduction/saturation. This type of representation allows the identification of classes of compounds such as aliphatics, aromatics, or highly oxidized compounds (Fig. 3).

The oxidation state of carbon allows the degree of oxidation of organic species (alcohols, aldehydes, carboxylic acids, esters, ethers, and ketones, but not peroxides) (Kroll et al., 2011) to be measured. It is defined by the simple equation:

$$OSc \approx 2O/C - H/C$$

This data can be used together with the atomic ratios of van Krevelen's diagrams to identify families of organic compounds (Tu et al., 2016;Wang et al., 2017a;Bianchi et al., 2019). In the case of HOMs, three families of compounds can be distinguished according to their oxidation state and the O/C and H/C ratios:

$O/C \geq 0.6$ and $OS_c \geq 0$ (Region 1, highly oxygenated and highly oxidized)

$O/C \geq 0.6$ and $OS_c < 0$ (Region 2, very oxygenated and moderately oxidized)

$OS_c \geq 0$ and $H/C \leq 1.2$ (Region 3, moderately oxygenated and highly oxidized)

4. Results and discussion

The oxidation of 1% limonene ($C_{10}H_{16}$) was studied at 590 K, atmospheric pressure, and at a residence time of 2 s. Under these conditions, the fuel conversion is moderate but formation of low-temperature oxidation products is maximized.

To study the nature of the chemical products formed and the particularity of auto-oxidation, we compared our results with those obtained by ozonolysis and OH-initiated photooxidation of limonene. This comparison was carried out using visualization methods adapted to large intrinsic data sets of high resolution and high sensitivity reached with current mass spectrometry. At this scale, these tools allow differentiating families of compounds or chemical processes that are hardly perceptible at the level of a few individuals (chemical species).

The comparison of the oxidation modes of limonene (auto-oxidation and ozonolysis/photooxidation) was based only on the nature of the chemical formula of products, without considering the quantitative, sensitivity, or ionization aspects that are difficult to exploit given the diversity of chemical products formed in this study (i) of the analytical methods, and (ii) the large number of instruments involved in this comparison.

To carry out this comparison, and in order to obtain the greatest representativeness of the oxidation of limonene by ozonolysis and OH-initiated photooxidation, we have selected nine previous studies for their diversity of oxidation and characterization processes. Table 1 presents the main experimental parameters of these studies.

https://doi.org/10.5194/acp-2020-1070
Preprint. Discussion started: 8 December 2020

Atmospheric Chemistry and Physics Discussions

Table 1. Main experimental parameters for studies of limonene oxidation.

Ref	Oxidation	Sampling	Experimental Setup	Initial concentrations of reactants	Ionization source	Instrument
(Fang et al., 2017)	OH-initiated photooxidation dark ozonolysis	online	smog chamber	500 ppb of ozone 900–1500 ppb of limonene	UV; 10 eV	Time-of-Flight (ToF)
(Witkowski and Gierczak, 2017)	Dark ozonolysis	off-line	flow reactor	0.15 to 4.0 ppm ozone Limonene concentration not provided	ESI; 4.5 kV	Triple quadrupole
(Jokinen et al., 2015)	Ozonolysis	online	flow glass tube	6.1-6.9 $x10^{11}$molec.cm^{-3} of ozone 1–10000 $x10^{9}$molec.cm^{-3} of limonene	chemical ionization	Time-of-Flight (ToF)
(Nørgaard et al., 2013)	Ozone (plasma)	online	Direct on the support	850 ppb ozone 15-150 ppb limonene	plasma	Quadrupole time-of-flight (QToF)
(Bateman et al., 2009)	Dark and UV radiations ozonolysis	off-line	Teflon FEP reaction chamber	1 ppm ozone 1 ppm limonene	ESI; (not specified)	LTQ-Orbitrap Hybrid Mass Spectrometer
(Walser et al., 2008)	Dark ozonolysis	off-line	Teflon FEP reaction chamber	1-10 ppm ozone 10 ppm limonene	ESI; 4.5 kV	LTQ-Orbitrap Hybrid Mass Spectrometer
(Warscheid and Hoffmann, 2001)	Ozonolysis	online	Smog chamber	300-500 ppb ozone and limonene	APCI; 3kV	Quadrupole ion trap mass spectrometer
(Hammes et al., 2019)	Dark ozonolysis	online	Flow reactor	400-5000 ppb ozone 15, 40, 150 ppb of limonene	^{210}Po alpha	HR-ToF-CIMS
(Kundu et al., 2012)	Dark ozonolysis	off-line	Teflon reaction chamber	250 ppb ozone 500 ppb limonene	ESI; 3.7 and 4 kV	LTQ FT Ultra, Thermo Scientific
This work	Cool-flame auto-oxidation	off-line	Jet-stirred reactor	1% limonene 56 %O_2, 43 %N_2	APCI; 3kV HESI; 3.8 kV	Orbitrap® Q-Exactive

These nine experimental studies yielded a first set of 1233 molecules for an inventory which, although incomplete, gives a broad representativeness of the chemical products resulting from limonene ozonolysis and OH-initiated photooxidation.

https://doi.org/10.5194/acp-2020-1070
Preprint. Discussion started: 8 December 2020

Atmospheric Chemistry and Physics Discussions

The second set was obtained using the chemical formulae observed here during limonene auto-oxidation. For the identification phase, we favored direct injection for its sensitivity. We used UHPLC for its capacity of isomers separation and advanced isomers identification through MS-MS analysis. For direct injection, we have chosen a HESI source operating in negative mode (3.8 kV, sheath gas :12, T capillary vaporizer temperature: 120°C, mass range between 50 and 1000 Da) for its wide range of polar molecule ionization. After verification of the absence of oxidation induced by the ionization source (Pasilis et al., 2008;Chen and Cook, 2007) and elimination of the ions common to the reference, attribution rules were made on the basis of molecules composed solely of carbon, hydrogen and oxygen, respecting a deviation of less than 3 ppm by mass over the range 50-1000 Da. Chemical formula with relative intensity was less than 1 ppm were not considered. Following these rules, we identified 1138 chemical formula in our oxidized limonene sample, which we split into three groups centred on the number of monomers, i.e. a limonene molecule with different degrees of oxidation: I (50<m/z<300); II (300<m/z<500) and III (500<m/z<700) (Kundu et al., 2012;Leungsakul et al., 2005;Nørgaard et al., 2013).

These groups are identified in Figure 1 which shows the mass spectrum of oxidized limonene. Generally speaking, these groups are built around one or more monomers and a few families of chemical reactions. Group I corresponds to compounds resulting from multiple oxidation reactions including fragmentation and condensation. Groups II and III correspond to higher molecular masses, resulting from addition and condensation reactions including, in the case of ozonolysis reactions of (i) hemiacetalization, (ii) with radicals (hydroperoxy or Griegee), and (iii) of condensation of aldols and/or esterification (Kundu et al., 2012).

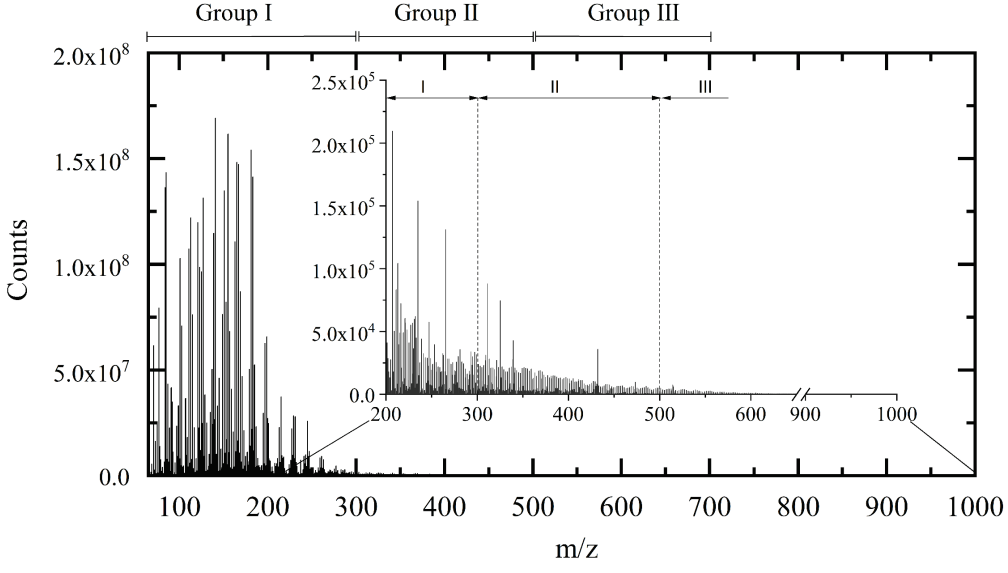

Figure 1. Limonene oxidation sample analyzed by FIA and HESI (sheath 12, aux gas 0, voltage 3.8kV, $T_{capillary}$ vaporizer temperature120°C).

https://doi.org/10.5194/acp-2020-1070
Preprint. Discussion started: 8 December 2020

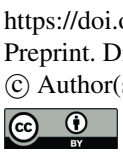

Atmospheric Chemistry and Physics Discussions

The two sets obtained from each oxidation mode were merged, forming a new set of 1600 molecules. In this set, ~50% of the chemical formulae (771) are common to both oxidation modes, while 462 molecular formulae are obtained solely by ozonolysis/ photooxidation and 367 are produced in auto-oxidation experiments only.

All the molecular formulae were represented in a Kendrick diagram (based on a CH_2 structural unit) associated with the DBE number (Fig. 2). The representation of Kendrick highlights the families of compounds, the addition of a third dimension makes it possible to study the reaction mechanisms linking these different families (Bateman et al., 2009); (Kundu et al., 2012).

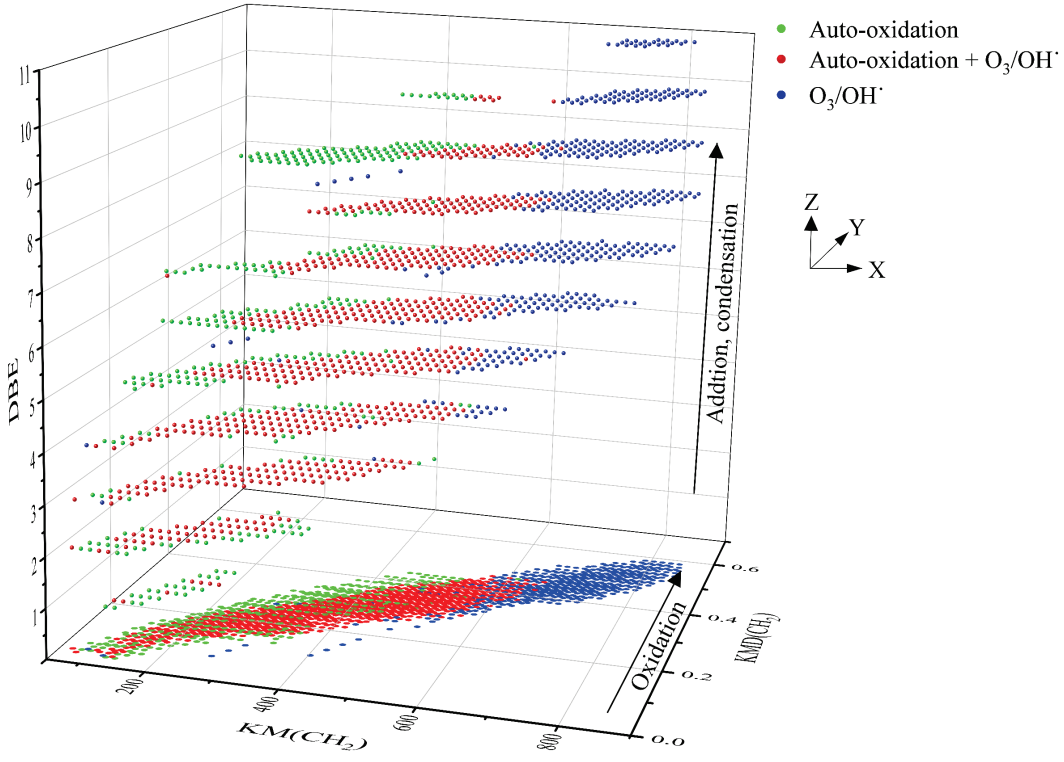

Figure 2. All the chemical products, resulting from limonene oxidation by ozonolysis/photooxidation and auto-oxidation gathered in the form of a Kendrick diagram correlated to the DBE (with projection on the XY plane): ● new chemical products from auto-oxidation experiments (JSR) ● common to the 3 modes of oxidation ● chemical products with molecular formulae not observed in auto-oxidation.

https://doi.org/10.5194/acp-2020-1070
Preprint. Discussion started: 8 December 2020


Atmospheric Chemistry and Physics Discussions

The chemical formulae are distributed into 11 XY planes according to their DBE number. The representation of each of these XY plans is given in the S1 supplementary material. This representation immediately highlights the origin of the chemical formulae, i.e. those specific to auto-oxidation, common to the three modes of oxidation, or specific to ozonolysis and photooxidation. The chemistry of these chemical species can then be read graphically on the axes: the X-axis represents the extent of the family, the Y-axis represents oxidation and the Z-axis denotes addition and condensation reactions. This is illustrated in Figure S1 of the Supplementary material.

Unexpectedly, the distribution of chemical formulae is homogeneous and forms a continuum between oxidation by auto-oxidation and by ozonolysis/photooxidation.

In auto-oxidation, the above mentioned pathways, probably constrained by short oxidation time (residence time of 2 s), seem to extend the molecular weight growth of products up to ~300 Da, favor splitting (decrease of DBE), additions or condensation (increase of DBE) of unsaturated chemical groups. Ozonolysis and photooxidation experiments, performed over longer periods of time (several seconds < t < few hours), promote, in addition to the previous reactions, the appearance of oligomers and an increase of products molecular weight (Zhao et al., 2015).

In the Kendrick diagram (Fig.2), the DBE=3 XY plane containing limonene includes chemical formulae of products deriving from the early oxidation steps. In this case, the breaking of unsaturation, double bond, and ring are counterbalanced by the formation of carbonyls or ozonides, keeping DBE constant. In this XY plane, 83% of the chemical formulae of products obtained by auto-oxidation are identical to those formed by ozonolysis/photooxidation, although ozone is most likely absent from JSR auto-oxidation experiments. Many of the chemical formulae of products described in previous ozonolysis/photooxidation works involve reaction mechanisms based on ozonides and Criegee intermediates. These chemicals can be primary products, i.e. weakly oxidized (Bateman et al., 2009) ($C_9H_{14}O_3$, $C_9H_{14}O_4$, $C_{10}H_{14}O_3$, $C_{10}H_{14}O_4$, $C_{10}H_{16}O_2$, $C_{10}H_{16}O_3$, $C_{10}H_{16}O_4$) but also secondary, with an increasing number of oxygen atoms ($C_7H_{10}O_4$, $C_7H_{10}O_5$, $C_8H_{12}O_3$, $C_8H_{12}O_4$, $C_8H_{12}O_5$, $C_9H_{14}O_3$, $C_9H_{14}O_4$, $C_9H_{14}O_5$, $C_{10}H_{16}O_3$) (Hammes et al., 2019) and ($C_7H_{10}O_6$, $C_8H_{12}O_6$, $C_9H_{14}O_6$) (Kundu et al., 2012). The new chemical formulae of products detected do not form a new group, but are in the continuity of the families of chemical molecules found in previous studies (Witkowski and Gierczak, 2017;Jokinen et al., 2015;Walser et al., 2008;Kundu et al., 2012;Fang et al., 2017;Nørgaard et al., 2013;Bateman et al., 2009;Warscheid and Hoffmann, 2001;Hammes et al., 2019). These families are built on the basis of a simple difference in alkyl groups (CH_2 basic unit of the Kendrick diagram).

The decrease of DBE from 3 to 2 and then to 1 reflects a greater reactivity on double bonds and on the limonene ring. This reactivity on unsaturated sites is accompanied by a fragmentation of the C-C bonds and a decrease in molecular weight. The new molecular formula of products, specific to auto-oxidation, are located at the extremities of the DBE=2 plane or on almost the entire DBE=1 plane. They are characterized by a lower O/C ratio, which can be explained by less advanced oxidation, and certainly by fragmentation. The observation of these new chemical formulae of products, compared to previous studies, can be explained, in addition to the short oxidation time and the elevated temperature in the JSR experiment, by a termination in the radical chain process or by bimolecular reactions (Rissanen et al., 2014;Walser et al., 2008).

https://doi.org/10.5194/acp-2020-1070
Preprint. Discussion started: 8 December 2020

Atmospheric Chemistry and Physics Discussions

The increase in DBE from 3 to 11 characterizes the increase in double bonds and degree of unsaturation obtained by the addition or condensation of limonene oxidized species. In the case of ozonolysis/photooxidation, this increase is usually explained by reactions between Criegee radicals (Criegee intermediate) and acids or alcohols, by hemiacetal formation, aldolization, or esterification (Bateman et al., 2009;Docherty et al., 2005). Each of these reactions is associated with an increase in DBE (hemiacetal: +2; aldolization: +3). For example, in the case of aldol condensation between two aldehydes (limonoaldehyde + 7-OH-limonoaldehyde), the DBE increases from 3 to 6. The emergence of new chemical formulae of products with DBE=9 is mostly observed for molecular weights between 200 and 500 Da. These molecules probably correspond to the addition or condensation of several oxidized limonene compounds (condensation/addition of several cycles) favored, under short time oxidation, by the elevated experimental temperature (590 K).

In general, the new molecular formulae of products observed in auto-oxidation, compared to ozonolysis (Tu et al., 2016), have a lower molecular weight and are better found in group I (m/z < 300, 52%) associated with addition or splitting reactions around the limonene skeleton (monomer channel).

In ozonolysis/photooxidation, the products which molecular formulae are rather located in groups II and III can easily oligomerize. This process is highly time-dependent in the presence of ozone (Kundu et al., 2012).

In addition to the identification of chemical families by Kendrick's analysis, it is possible to specify the nature of the chemical products using a van Krevelen diagram. Figure 3 shows a representation of all the chemical formulae of products observed in this work, overlayed on the locations of the different families of chemical compounds described in the literature (Bianco et al., 2018;Nozière et al., 2015). These families are defined by O/C and H/C ratios and shown in Figure 3.

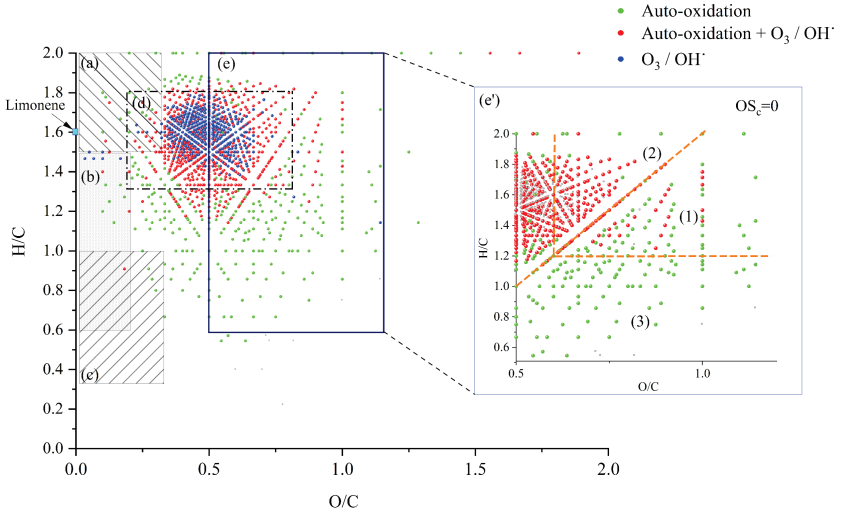

Figure 3. van Krevelen representation of all the chemical products and the different families of chemical compounds described in the literature: (a) aliphatics compounds; (b) aromatics hydrocarbons; (c) unsaturated hydrocarbons; (d) compounds obtained by ozonolysis (including OH-initiated oxidation) (Kundu et al., 2012); (e) HOMs, (e') HOMs formed without O_3/OH·.

https://doi.org/10.5194/acp-2020-1070
Preprint. Discussion started: 8 December 2020

Atmospheric Chemistry and Physics Discussions

In the limonene oxidation process, observable from the left to the right on this figure, the first oxidation steps concern both the products resulting from JSR auto-oxidation and those from ozonolysis/photooxidation.

4.1 Characterization of KHPs

Oxidation, at the initial stage, forms compounds with number of carbon atoms varying from 7 to 11, number of hydrogen atoms ranging from 12 to 16, and number of oxygen atoms increasing to 9. These chemical compounds are globally in the (d) area. In ozonolysis/photooxidation studies, initial oxidation phase, by ozone and/or the radical $OH^{\cdot}$ have been widely described (Walser et al., 2008;Kundu et al., 2012;Nørgaard et al., 2013;Librando and Tringali, 2005). Although the experimental conditions and the associated reaction mechanisms are different, it is observed, similarly to Fang et al (Fang et al., 2017), many common products of these different oxidation modes. In the case of auto-oxidation, in the absence of ozone, H-abstraction by the radical $OH^{\cdot}$ initiates further oxidation steps yielding $ROO^{\cdot}$ radicals and hydroperoxides.

$$RH + OH \leftrightarrows R^{\cdot} + H_2O \; ; \; R^{\cdot} + O_2 \leftrightarrows ROO^{\cdot} \; ; \; ROO^{\cdot} + R'H \leftrightarrows ROOH + R'$$

These reactions will themselves lead to the formation of, among others, KHPs, diketones, or will proceed further (see Section 1) and lead to the formation of HOMs (Jokinen et al., 2014b;Wang et al., 2019;Wang et al., 2016). In the initial stage of this autooxidation, we studied the formation of the compounds $C_{10}H_{14}O_3$, $C_{10}H_{12}O_2$, $C_{10}H_{16}O_2$, $C_{10}H_{14}O_{5\text{-}11}$ corresponding respectively to the global formulae of KHPs, diketones, oxyhydroxides, and HOMs. Experiments were carried out using UHPLC-Orbitrap coupling in tandem mode in order to isolate these molecules and fragment them with an HCD at energy ranging from 10 to 30 eV. Considering a mass range of initial molecules detected in auto-oxidation lower than 700 Da, we used an APCI source in positive mode, well suited to this mass range.

For the KHPs ($C_{10}H_{14}O_3$), whose mechanisms of formation from limonene are described in the Supplementary material S4 (with example of reaction mechanisms of KHP formation and probable sites of attack of OH radicals), the analyses by high resolution mass spectrometry confirm the presence of 12 isomers among the compounds formed, compared to a maximum of 18 potentially produced (S5).

Among these 12 isomers, MS/MS fragmentation allowed the identification of three groups of compounds presented in Figure 4. The limits of separation and detection of these chemical compounds made it impossible to specify the position of the functional groups in these isomers.

https://doi.org/10.5194/acp-2020-1070
Preprint. Discussion started: 8 December 2020

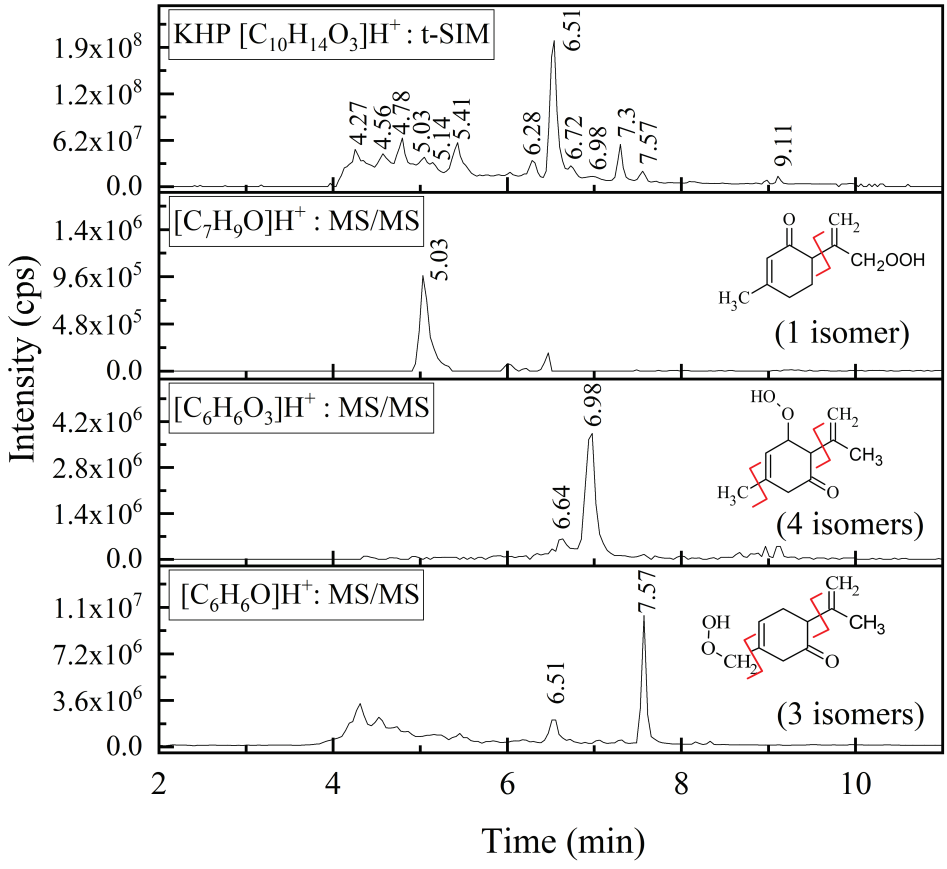

Figure 4. MS analyses of the KHPs isomers together with their fragmentation and number of possible isomers for each group (S5).

In order to verify the presence of carbonyl groups, 20 µl of a mixture containing DNPH (20 µl of H_3PO_4 (85%) in ACN with 20 µl of 2,4-DNPH) were added to 1 ml of sample. This mixture was allowed to react for 4 hours before analysis. Characterization, at different reaction times (0.5, 1, and 4 hours), was performed by UHPLC-MS APCI ($^-$) in tSIM mode following 361.1153 Da mass of the $C_{16}H_{18}O_6N_4$ compound (Fig. S6). One could note an increase in the intensity of the signal (inset Fig. S6). Nearly 12 isomers were observed, with an elution time that is longer and consistent with the initial retention time of the KHPs, thus confirming the presence of carbonyl groups. However, the fragmentation carried out on all these chromatographic peaks did not make it possible to complete the chemical speciation of all the isomers. Nevertheless, for the first time, this study confirms the formation of KHPs initiated by the $OH^{\cdot}$ radical during the oxidation of limonene.

The difficulty for characterizing KHPs lies in the fact that these products are unstable and transform according to different mechanisms. One of the instabilities described in the literature consists in spontaneous dehydration of KHPs to give diketones

https://doi.org/10.5194/acp-2020-1070
Preprint. Discussion started: 8 December 2020

Atmospheric Chemistry and Physics Discussions

(Herbinet et al., 2012). Analysis of the data confirms the presence of a diketone ($C_{10}H_{12}O_2$). It shows that diketones are detected both by elution of oxidized limonene (7.79 and 8 min), and systematically in the chromatogram of KHP isomers. This means that this spontaneous transformation can occur in the spectrometer without questioning the presence of diketones in the initial sample. Figure S7 in the Supplementary material compares the two profiles of diketones resulting from the fragmentation of KHPs and by elution.

Other transformation pathways of KHPs are possible, e.g., via the Korcek mechanism (Mutzel et al., 2015) where δ-KHPs decompose into carbonyl compounds and carboxylic acids. Among the 18 proposed KHPs (Supplementary material S5), 4 isomers (#4, 11, 15, and 18) could react via the Korcek mechanism, but only the #4 isomer is likely to form a cyclic peroxide between a carbonyl group and a hydroperoxide group. The other three isomers will give, after ring opening, isomers of the compound $C_{10}H_{14}O_3$. For the #4 isomer, the Korcek mechanism leads to the formation of a carbonyl compound, $C_9H_{12}O$, and the formic acid CH_2O_2 (Fig. 5). UHPLC analyses confirm the presence of products with chemical formula $C_9H_{12}O$ in the form of two isomers (Fig. 5), but only the peak located at 5.64 minutes shows a C_8H_{12} fragment consistent with the transformation of the initial KHP.

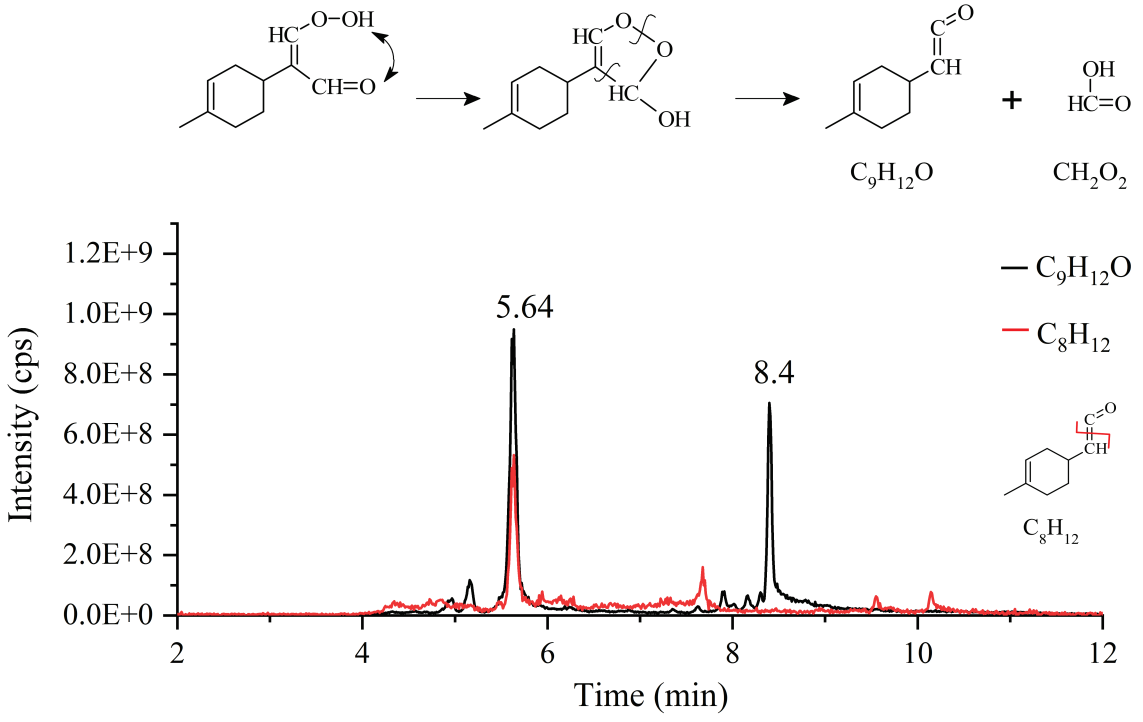

Figure 5. Korcek mechanism for the #4 KHP isomer and chromatograms of $C_9H_{12}O$ and the fragment C_8H_{12} (APCI(+), vaporizer temperature =120°c, sheath gas flow of 50 a.u., auxiliary gas flow of 0 a.u.; sweep gas flow of 0 a.u., capillary temperature of 300°C, corona current of 3 μA).

https://doi.org/10.5194/acp-2020-1070
Preprint. Discussion started: 8 December 2020

Atmospheric Chemistry and Physics Discussions

KHPs can also give rise to branching reactions that will generate radicals promoting autoxidation by OH˙ (Wang et al., 2016).

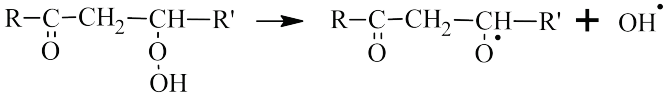

Otherwise, if the H-atom transfer in the OOQOOH intermediate does not involve the H-C-OOH group but another H-C group, then no ketohydroperoxide is formed and a third O_2 addition to HOOQ'OOH yielding OOQ'$(OOH)_2$ can occur. If oxidation proceeds further following this pathway, it can lead to the formation of HOMs.

4.2 Characterization of HOMs

Different strategies were considered for tracking the production of HOMs. Because of higher sensitivity and difficulty in separating isomers, FIA was preferred. The compounds $C_{10}H_{14}O_5$, $C_{10}H_{14}O_7$, $C_{10}H_{14}O_9$, $C_{10}H_{14}O_{11}$ (Fig. 3, area (d)) were detected by FIA (APCI positif, vaporizer temperature =120°C, sheath gas flow of 12 a.u., auxiliary gaz flow of 0 a.u.; sweep gas flow of 0 a.u., capillary temperature of 300°C, corona discharge current of 3 µA, flow of 8 µl/min). Nevertheless, the diversity of reaction pathways, associated with the increasing number of chemical compounds, makes it difficult within a population of several hundred chemical compounds to identify all HOMs.

We have therefore again used the van Krevelen diagram, which allows following the evolution of the oxidation of the first HOMs and to identify them according to definitions that seem to be consensus (Walser et al., 2008;Tu et al., 2016;Nozière et al., 2015;Wang et al., 2017a). To this end, we used the average carbon oxidation state OS_c which allows distinguishing three regions according to the nature of the functional groups: Region 1 ($O/C \geq 0.6$ and $OS_c \geq 0$) consists of highly oxygenated and highly oxidized compounds (acids and carbonyls), Region 2 ($O / C \geq 0.6$ and $OS_c < 0$), consists of highly oxygenated and moderately oxidized compounds (alcohols, esters and peroxides), finally, Region 3 ($OS_c \geq 0$ and $H/C \leq 1.2$) includes compounds with a moderate level of oxygen, but strongly oxidized (Tu et al., 2016).

It can be seen from Figure 3 that auto-oxidation enhances the development of HOMs, compared to ozonolysis/photooxidation, and that the majority of these new products are found in Regions 1 and 3 of the inset of Figure 3. Thus, further oxidation can go on. We observed products of addition of up to 17 oxygen atoms yielding $C_{25}H_{32}O_{17}$.

Considering the presence of the radicals OH˙, we also searched for chemical compounds resulting from the Waddington mechanism (Li et al., 2020). This mechanism, through which oxidation of alkenes can occur, has two reaction pathways in the case of limonene. The first pathway leads to the formation of a $C_9H_{14}O$ ketone and formaldehyde via oxidation of the exocyclic double bond. The second, involving the endocyclic double bond of limonene, gives the compound $C_{10}H_{16}O_2$. For each pathway, we obtained three isomers on the chromatograms (Fig. 6).

https://doi.org/10.5194/acp-2020-1070
Preprint. Discussion started: 8 December 2020

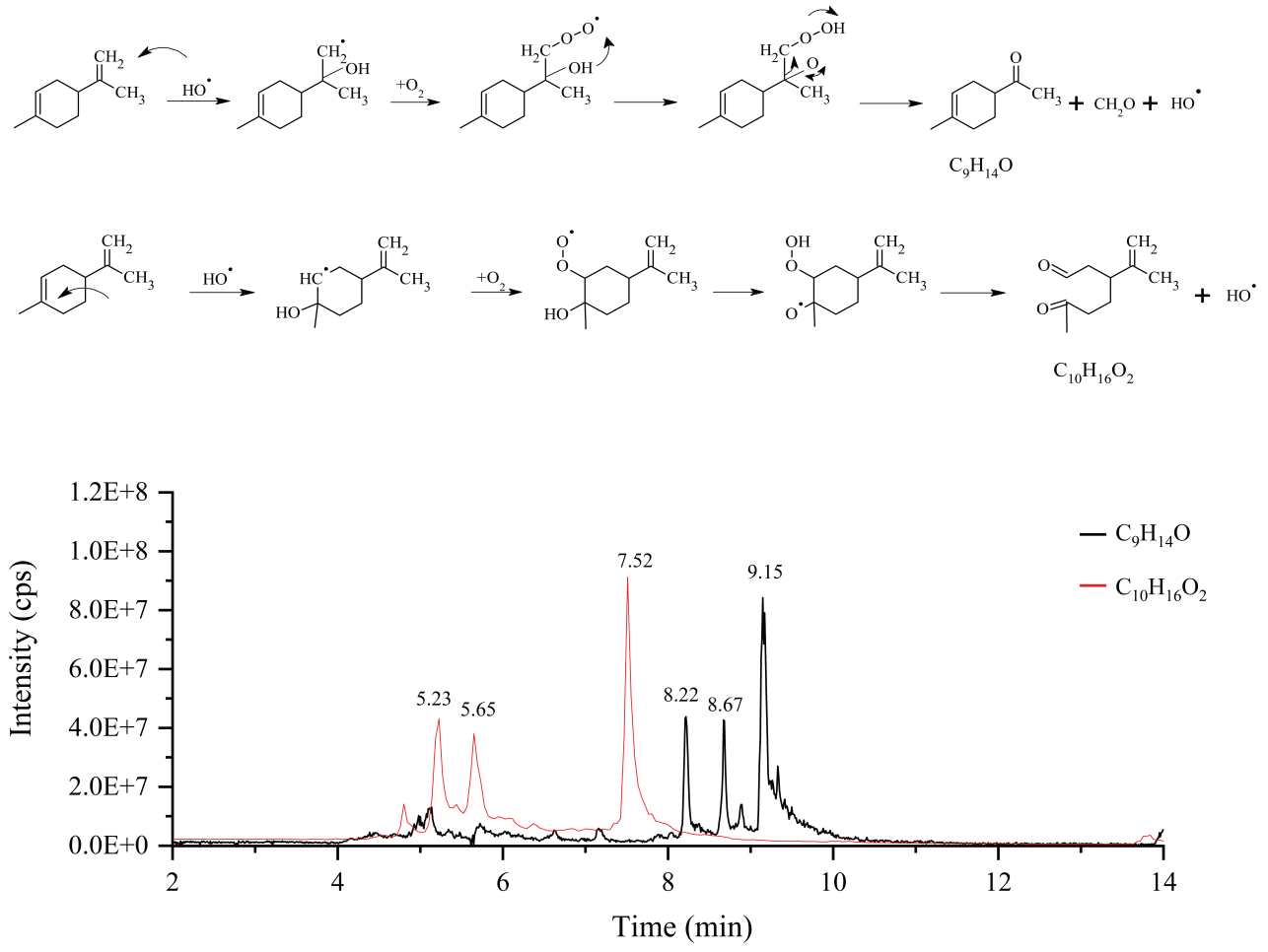

Figure 6. Oxidation of limonene according to the Waddington mechanism and chromatograms of the compounds obtained: $C_9H_{14}O$ and $C_{10}H_{16}O_2$ ($APCI^+$)

345

The fragmentation of these isomers did not allow their identification. However, in order to confirm the presence of carbonyl groups, we added 20 µl of a mixture containing DNPH (Same experimental condition as above) to 1 ml of sample, and let this mixture react for 4 hours before analyses. In order to facilitate the detection of isomers and their addition compounds, we used the APCI(-) mode for UHPLC analyses. Only the compound C16H20O5N4 (C10H16O2 + DNPH) was detected. The second
350 carbonyl compound (yielding C22H24O8N8) could not be confirmed (Supplement SI fig. 8). Moreover, the addition of D2O, in order to test the presence of -OH or -OOH groups, gave no results for the two chemical compounds. Recent modelling work on Waddington mechanism (Lizardo-Huerta et al., 2016) has shown that structural parameters have an impact on the energy

https://doi.org/10.5194/acp-2020-1070
Preprint. Discussion started: 8 December 2020

Atmospheric Chemistry and Physics Discussions

barriers associated with the β-scission step. There, a decrease in the activation energy is observed when the substitution of the carbon atom carrying the peroxyl function increases. According to that study, this effect is amplified by the degree of substitution of the carbon atom carrying the hydroxy group. These results are in agreement with the preferential detection of the compound $C_{10}H_{16}O_2$ whose carbon atoms, with the peroxy groups, is the most substituted. Beyond the complete identification of the isomers, this study confirms the presence of chemical compounds which could well result from the Waddington mechanism during limonene auto-oxidation in JSR.

4.3 Complementary method of screening

Further study of the oxidation of chemical compounds and their reaction mechanisms is limited by the complexity of the exponential increase of chemical reactions, chemical species, and their isomers. Nevertheless, monitoring the evolution of these complex mixtures is possible by correlating the OSc to the number of carbon atoms (n_c). We have reported in Figure 7 our measurements and have associated to these results the different biogenic VOCs families defined in the literature (Low-volatility oxygenated organic aerosol (LV-OOA), semi-volatile oxygenated organic aerosol (SV-OOA), hydrocarbon-like organic aerosol (HOA), and biomass burning organic aerosol (BBOA) corresponding to particulates (Kroll et al., 2011;An et al., 2019)). The development of advanced oxidation, specific to auto-oxidation, is confirmed with an OS_c close to 1. As it stands, it is difficult to make hypotheses on the evolution of these new chemical products and, in the absence of speciation, to assess their environmental impact.

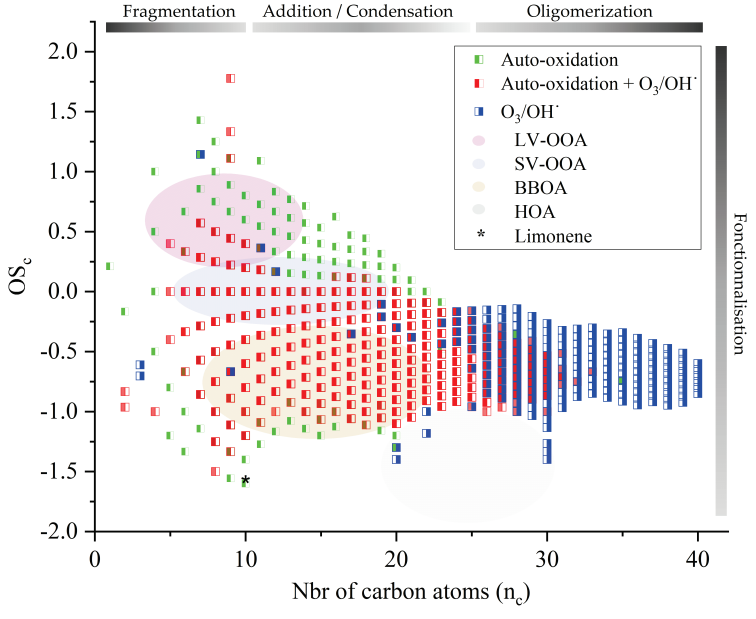

Figure 7. Representation in the OS_c-n_c space of all the chemical formulae considered in this study and analysis of the degree of oxidation.

https://doi.org/10.5194/acp-2020-1070
Preprint. Discussion started: 8 December 2020

Atmospheric Chemistry and Physics Discussions

Finally, it is also possible to further exploit the van Krevelen diagram by introducing reaction mechanisms. Until now this diagram has been used to identify reaction pathways or families of compounds (Kim et al., 2003;Wu et al., 2004). One can refine this identification by associating to a reaction mechanism a vector whose amplitude and direction will allow linking reagents and products. By applying this method to all the experimental data points, one scans the space of the possibilities of formation of a compound or its isomers.

If this method is applied to the formation of $C_{10}H_{14}O_3$ (KHPs and isomers), the vector is defined by the loss of two hydrogen atoms and the gain of three oxygen atoms. By focusing only on molecules composed of 10 carbon atoms, 31 $C_{10}H_{14}O_3$ isomers were identified, 17 of which are new chemical formulae detected in auto-oxidation only. This is an exhaustive inventory of the possibilities of formation of these compounds based on the experimental data points and not on thermodynamic and kinetic considerations. Applying the same method to the search for keto-dihydroperoxides (-2H; +5O) and di-ketohydroperoxide (-2H; +7O), we observed the formation of 24 and 23 compounds, respectively. All these results are presented in Figure 8.

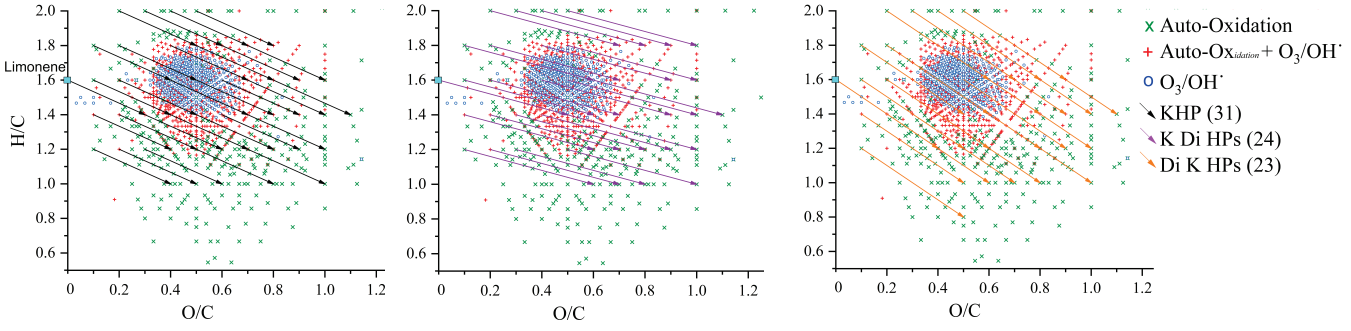

Figure 8. representation in the van Krevelen diagram of the vectors associated with reaction mechanisms for the formation of KHPs, keto-di-hydroperoxides (K Di HPs), and di-ketohydroperoxides (Di K HPs).

Thanks to all the tools used in this work, especially the last one, the screening of selected classes of compounds is considerably simplified, and the mesh constituted by the reaction vectors becomes a new method for evaluating the nature of a mixture of oxidation products.

5. Conclusion and perspectives

Numerous studies on the ozonolysis of limonene have allowed characterizing the reaction mechanisms of its oxidation by describing a large fraction of chemical products. In these mechanisms, the formation of a Criegee intermediate has often been described as the major pathway for the formation of oxidized compounds, associated with the more restricted formation of the OH˙ radical.

https://doi.org/10.5194/acp-2020-1070
Preprint. Discussion started: 8 December 2020

Among these studies, some have shown that despite these differences in oxidation mechanisms of ozonolysis, many of the products were similar. Moreover, it appears that these similarities are extended to photooxidation.

In the present study, where the comparison of oxidation modes is extended to auto-oxidation, we find, in the case of limonene, similar chemical products (nearly 50%). It appears that in the absence of ozone, the oxidation by the OH˙ radical, common to ozonolysis, gives similar results. Nevertheless, this study has allowed us to highlight auto-oxidation specific processes, such as formation of KHPs and diketones, occurrence of the Korcek and Waddington reaction mechanisms.

Analysis at the molecular level was complemented by observation at chemical family scale using Kendrick and van Krevelen visualization tools, necessary to compare and identify features in large data sets. Indeed, the formation of new HOMs and the development of combustion-related auto-oxidation are perfectly perceptible using these tools. The same is true for the oligomerization, which is not very important in auto-oxidation, in favor of addition and/or condensation reactions on limonene that are prompt to increase the DBE. As it stands, the meshing within these chemical families according to reaction, thermodynamic, or kinetic criteria remains sketchy, but will certainly develop in the light of all the available experimental and theoretical inputs. Further studies involving others terpenes are underway. They should confirm the results presented here.

Acknowledgments

The authors gratefully acknowledge funding from Labex Caprysses (ANR-11-LABX-0006-01), the Labex Voltaire (ANR-10-LABX-100-01), and financial support from CPER and EFRD (PROMESTOCK and APPROPOR-e projects).

References

An, Y., Xu, J., Feng, L., Zhang, X., Liu, Y., Kang, S., Jiang, B., and Liao, Y.: Molecular characterization of organic aerosol in the Himalayas: insight from ultra-high-resolution mass spectrometry, Atmos. Chem. Phys., 19, 1115-1128, 10.5194/acp-19-1115-2019, 2019.

Bateman, A. P., Nizkorodov, S. A., Laskin, J., and Laskin, A.: Time-resolved molecular characterization of limonene/ozone aerosol using high-resolution electrospray ionization mass spectrometry, Physical Chemistry Chemical Physics, 11, 7931-7942, 10.1039/B905288G, 2009.

Belhadj, N., Benoit, R., Dagaut, P., Lailliau, M., Serinyel, Z., Dayma, G., Khaled, F., Moreau, B., and Foucher, F.: Oxidation of di-n-butyl ether: Experimental characterization of low-temperature products in JSR and RCM, Combustion and Flame, 222, 133-144, 10.1016/j.combustflame.2020.08.037, 2020.

Belhadj, N., Benoit, R., Dagaut, P., Lailliau, M., Serinyel, Z., and Dayma, G.: Oxidation of di-n-propyl ether: Characterization of low-temperature products, Proc. Combust. Inst., 38, 10.1016/j.proci.2020.06.350, 2020.

Benson, S. W.: The kinetics and thermochemistry of chemical oxidation with application to combustion and flames, Progress in Energy and Combustion Science, 7, 125-134, 10.1016/0360-1285(81)90007-1, 1981.

Berndt, T., Richters, S., Kaethner, R., Voigtlaender, J., Stratmann, F., Sipilae, M., Kulmala, M., and Herrmann, H.: Gas-phase ozonolysis of cycloalkenes: Formation of highly oxidized RO2 radicals and their reactions with NO, NO2, SO2, and other RO2 adicals, J. Phys. Chem. A, 119, 10336, 10.1021/acs.jpca.5b07295, 2015.

https://doi.org/10.5194/acp-2020-1070
Preprint. Discussion started: 8 December 2020

Berndt, T., Richters, S., Jokinen, T., Hyttinen, N., Kurtén, T., Otkjær, R. V., Kjaergaard, H. G., Stratmann, F., Herrmann, H., Sipilä, M., Kulmala, M., and Ehn, M.: Hydroxyl radical-induced formation of highly oxidized organic compounds, Nature Communications, 7, 13677, 10.1038/ncomms13677, 2016.

Bianchi, F., Kurtén, T., Riva, M., Mohr, C., Rissanen, M. P., Roldin, P., Berndt, T., Crounse, J. D., Wennberg, P. O., Mentel, T. F., Wildt, J., Junninen, H., Jokinen, T., Kulmala, M., Worsnop, D. R., Thornton, J. A., Donahue, N., Kjaergaard, H. G., and Ehn, M.: Highly Oxygenated Organic Molecules (HOM) from Gas-Phase Autoxidation Involving Peroxy Radicals: A Key Contributor to Atmospheric Aerosol, Chemical Reviews, 119, 3472-3509, 10.1021/acs.chemrev.8b00395, 2019.

Bianco, A., Deguillaume, L., Vaïtilingom, M., Nicol, E., Baray, J.-L., Chaumerliac, N., and Bridoux, M.: Molecular Characterization of Cloud Water Samples Collected at the Puy de Dôme (France) by Fourier Transform Ion Cyclotron Resonance Mass Spectrometry, Environmental Science & Technology, 52, 10275-10285, 10.1021/acs.est.8b01964, 2018.

Chen, M., and Cook, K. D.: Oxidation artifacts in the electrospray mass spectrometry of A beta peptide, Anal. Chem., 79, 2031-2036, 10.1021/ac061743r, 2007.

Cox, R. A., and Cole, J. A.: Chemical aspects of the autoignition of hydrocarbon-air mixtures, Combust. Flame, 60, 109-123, 10.1016/0010-2180(85)90001-X, 1985.

Crounse, J. D., Nielsen, L. B., Jørgensen, S., Kjaergaard, H. G., and Wennberg, P. O.: Autoxidation of Organic Compounds in the Atmosphere, The Journal of Physical Chemistry Letters, 4, 3513-3520, 10.1021/jz4019207, 2013.

Dagaut, P., Cathonnet, M., Rouan, J. P., Foulatier, R., Quilgars, A., Boettner, J. C., Gaillard, F., and James, H.: A Jet-Stirred Reactor for Kinetic-Studies of Homogeneous Gas-Phase Reactions at Pressures up to 10-Atmospheres (~ 1 MPa), Journal of Physics E-Scientific Instruments, 19, 207-209, 10.1088/0022-3735/19/3/009, 1986.

Dagaut, P., Daly, C., Simmie, J. M., and Cathonnet, M.: The oxidation and ignition of dimethylether from low to high temperature (500-1600 K): Experiments and kinetic modeling, Symposium (International) on Combustion, 27, 361-369, 10.1016/S0082-0784(98)80424-4, 1998.

Dagaut, P., and Lecomte, F.: Experiments and kinetic modeling study of NO-reburning by gases from biomass pyrolysis in a JSR, Energy Fuels, 17, 608-613, 10.1021/ef020256l, 2003.

Dayma, G., Togbe, C., and Dagaut, P.: Experimental and Detailed Kinetic Modeling Study of Isoamyl Alcohol (Isopentanol) Oxidation in a Jet-Stirred Reactor at Elevated Pressure, Energy Fuels, 25, 4986-4998, 10.1021/ef2012112, 2011.

Docherty, K. S., Wu, W., Lim, Y. B., and Ziemann, P. J.: Contributions of organic peroxides to secondary aerosol formed from reactions of monoterpenes with O-3, Environ. Sci. Technol., 39, 4049, 10.1021/es050228s, 2005.

Ehn, M., Thornton, J. A., Kleist, E., Sipilä, M., Junninen, H., Pullinen, I., Springer, M., Rubach, F., Tillmann, R., Lee, B., Lopez-Hilfiker, F., Andres, S., Acir, I.-H., Rissanen, M., Jokinen, T., Schobesberger, S., Kangasluoma, J., Kontkanen, J., Nieminen, T., Kurtén, T., Nielsen, L. B., Jørgensen, S., Kjaergaard, H. G., Canagaratna, M., Maso, M. D., Berndt, T., Petäjä, T., Wahner, A., Kerminen, V.-M., Kulmala, M., Worsnop, D. R., Wildt, J., and Mentel, T. F.: A large source of low-volatility secondary organic aerosol, Nature, 506, 476-479, 10.1038/nature13032, 2014.

Fang, W., Gong, L., and Sheng, L.: Online analysis of secondary organic aerosols from OH-initiated photooxidation and ozonolysis of α-pinene, β-pinene, Δ3-carene and d-limonene by thermal desorption–photoionisation aerosol mass spectrometry, Environmental Chemistry, 14, 75-90, 10.1071/EN16128, 2017.

Hammes, J., Lutz, A., Mentel, T., Faxon, C., and Hallquist, M.: Carboxylic acids from limonene oxidation by ozone and hydroxyl radicals: insights into mechanisms derived using a FIGAERO-CIMS, Atmos. Chem. Phys., 19, 13037-13052, 10.5194/acp-19-13037-2019, 2019.

Harvey, B. G., Wright, M. E., and Quintana, R. L.: High-Density Renewable Fuels Based on the Selective Dimerization of Pinenes, Energy Fuels, 24, 267-273, 10.1021/ef900799c, 2010.

Harvey, B. G., Merriman, W. W., and Koontz, T. A.: High-Density Renewable Diesel and Jet Fuels Prepared from Multicyclic Sesquiterpanes and a 1-Hexene-Derived Synthetic Paraffinic Kerosene, Energy Fuels, 29, 2431-2436, 10.1021/ef5027746, 2015.

Herbinet, O., Husson, B., Serinyel, Z., Cord, M., Warth, V., Fournet, R., Glaude, P.-A., Sirjean, B., Battin-Leclerc, F., Wang, Z., Xie, M., Cheng, Z., and Qi, F.: Experimental and modeling investigation of the low-temperature oxidation of n-heptane, Combustion and flame, 159, 3455-3471, 10.1016/j.combustflame.2012.07.008, 2012.

Hughey, C. A., Hendrickson, C. L., Rodgers, R. P., Marshall, A. G., and Qian, K.: Kendrick Mass Defect Spectrum: A Compact Visual Analysis for Ultrahigh-Resolution Broadband Mass Spectra, Analytical Chemistry, 73, 4676-4681, 10.1021/ac010560w, 2001.

https://doi.org/10.5194/acp-2020-1070
Preprint. Discussion started: 8 December 2020

Jensen, R. K., Korcek, S., Mahoney, L. R., and Zinbo, M.: Liquid-phase autoxidation of organic-compounds at elevated-temperatures .2. Kinetics and mechanisms of the formation of cleavage products in normal-hexadecane autoxidation, J. Am. Chem. Soc., 103, 1742-1749, 10.1021/ja00397a026, 1981.

Jokinen, T., Sipilä, M., Richters, S., Kerminen, V.-M., Paasonen, P., Stratmann, F., Worsnop, D., Kulmala, M., Ehn, M., Herrmann, H., and Berndt, T.: Rapid Autoxidation Forms Highly Oxidized RO2 Radicals in the Atmosphere, Angewandte Chemie International Edition, 53, 14596-14600, 10.1002/anie.201408566, 2014a.

Jokinen, T., Sipila, M., Richters, S., Kerminen, V. M., Paasonen, P., Stratmann, F., Worsnop, D., Kulmala, M., Ehn, M., and Herrmann, H.: Rapid autoxidation forms highly oxidized RO2 radicals in the atmosphere, Angew. Chem., Int. Ed., 53, 14596, 10.1002/anie.201408566, 2014.

Jokinen, T., Berndt, T., Makkonen, R., Kerminen, V.-M., Junninen, H., Paasonen, P., Stratmann, F., Herrmann, H., Guenther, A. B., Worsnop, D. R., Kulmala, M., Ehn, M., and Sipilä, M.: Production of extremely low volatile organic compounds from biogenic emissions: Measured yields and atmospheric implications, Proceedings of the National Academy of Sciences, 112, 7123, 10.1073/pnas.1423977112, 2015.

Kim, S., Kramer, R. W., and Hatcher, P. G.: Graphical Method for Analysis of Ultrahigh-Resolution Broadband Mass Spectra of Natural Organic Matter, the Van Krevelen Diagram, Analytical Chemistry, 75, 5336-5344, 10.1021/ac034415p, 2003.

Kourtchev, I., Giorio, C., Manninen, A., Wilson, E., Mahon, B., Aalto, J., Kajos, M., Venables, D., Ruuskanen, T., Levula, J., Loponen, M., Connors, S., Harris, N., Zhao, D., Kiendler-Scharr, A., Mentel, T., Rudich, Y., Hallquist, M., Doussin, J.-F., Maenhaut, W., Bäck, J., Petäjä, T., Wenger, J., Kulmala, M., and Kalberer, M.: Enhanced Volatile Organic Compounds emissions and organic aerosol mass increase the oligomer content of atmospheric aerosols, Scientific Reports, 6, 35038, 10.1038/srep35038, 2016.

Kourtchev, I., Szeto, P., O'Connor, I., Popoola, O. A. M., Maenhaut, W., Wenger, J., and Kalberer, M.: Comparison of Heated Electrospray Ionization and Nanoelectrospray Ionization Sources Coupled to Ultra-High-Resolution Mass Spectrometry for Analysis of Highly Complex Atmospheric Aerosol Samples, Analytical Chemistry, 92, 8396-8403, 10.1021/acs.analchem.0c00971, 2020.

Kroll, J. H., Donahue, N. M., Jimenez, J. L., Kessler, S. H., Canagaratna, M. R., Wilson, K. R., Altieri, K. E., Mazzoleni, L. R., Wozniak, A. S., Bluhm, H., Mysak, E. R., Smith, J. D., Kolb, C. E., and Worsnop, D. R.: Carbon oxidation state as a metric for describing the chemistry of atmospheric organic aerosol, Nat. Chem., 3, 133, 10.1038/nchem.948, 2011.

Kundu, S., Fisseha, R., Putman, A. L., Rahn, T. A., and Mazzoleni, L. R.: High molecular weight SOA formation during limonene ozonolysis: insights from ultrahigh-resolution FT-ICR mass spectrometry characterization, Atmos. Chem. Phys., 12, 5523-5536, 10.5194/acp-12-5523-2012, 2012.

Kune, C., McCann, A., Raphaël, L. R., Arias, A. A., Tiquet, M., Van Kruining, D., Martinez, P. M., Ongena, M., Eppe, G., Quinton, L., Far, J., and De Pauw, E.: Rapid Visualization of Chemically Related Compounds Using Kendrick Mass Defect As a Filter in Mass Spectrometry Imaging, Analytical Chemistry, 91, 13112-13118, 10.1021/acs.analchem.9b03333, 2019.

Leungsakul, S., Jeffries, H. E., and Kamens, R. M.: A kinetic mechanism for predicting secondary aerosol formation from the reactions of d-limonene in the presence of oxides of nitrogen and natural sunlight, Atmos. Environ., 39, 7063, 10.1016/j.atmosenv.2005.08.024, 2005.

Li, Y., Zhao, Q., Zhang, Y., Huang, Z., and Sarathy, S. M.: A Systematic Theoretical Kinetics Analysis for the Waddington Mechanism in the Low-Temperature Oxidation of Butene and Butanol Isomers, The Journal of Physical Chemistry A, 124, 5646-5656, 10.1021/acs.jpca.0c03515, 2020.

Librando, V., and Tringali, G.: Atmospheric fate of OH initiated oxidation of terpenes. Reaction mechanism of α-pinene degradation and secondary organic aerosol formation, Journal of Environmental Management, 75, 275-282, 10.1016/j.jenvman.2005.01.001, 2005.

Lizardo-Huerta, J. C., Sirjean, B., Bounaceur, R., and Fournet, R.: Intramolecular effects on the kinetics of unimolecular reactions of β-HOROO˙ and HOQ˙OOH radicals, Physical Chemistry Chemical Physics, 18, 12231-12251, 10.1039/C6CP00111D, 2016.

Llusia`, J., and Penuelas, J.: Seasonal patterns of terpene content and emission from seven Mediterranean woody species in field conditions, American Journal of Botany, 87, 133-140, 10.2307/2656691, 2000.

Meylemans, H. A., Quintana, R. L., and Harvey, B. G.: Efficient conversion of pure and mixed terpene feedstocks to high density fuels, Fuel, 97, 560-568, 10.1016/j.fuel.2012.01.062, 2012.

https://doi.org/10.5194/acp-2020-1070
Preprint. Discussion started: 8 December 2020

Morley, C.: A Fundamentally Based Correlation Between Alkane Structure and Octane Number, Combust. Sci. Technol., 55, 115-123, 10.1080/00102208708947074, 1987.
Mutzel, A., Poulain, L., Berndt, T., Iinuma, Y., Rodigast, M., Böge, O., Richters, S., Spindler, G., Sipilä, M., Jokinen, T., Kulmala, M., and Herrmann, H.: Highly Oxidized Multifunctional Organic Compounds Observed in Tropospheric Particles: A Field and Laboratory Study, Environmental Science & Technology, 49, 7754-7761, 10.1021/acs.est.5b00885, 2015.
Nørgaard, A. W., Vibenholt, A., Benassi, M., Clausen, P. A., and Wolkoff, P.: Study of Ozone-Initiated Limonene Reaction Products by Low Temperature Plasma Ionization Mass Spectrometry, Journal of The American Society for Mass Spectrometry, 24, 1090-1096, 10.1007/s13361-013-0648-3, 2013.
Nozière, B., Kalberer, M., Claeys, M., Allan, J., D'Anna, B., Decesari, S., Finessi, E., Glasius, M., Grgić, I., Hamilton, J. F., Hoffmann, T., Iinuma, Y., Jaoui, M., Kahnt, A., Kampf, C. J., Kourtchev, I., Maenhaut, W., Marsden, N., Saarikoski, S., Schnelle-Kreis, J., Surratt, J. D., Szidat, S., Szmigielski, R., and Wisthaler, A.: The Molecular Identification of Organic Compounds in the Atmosphere: State of the Art and Challenges, Chemical Reviews, 115, 3919-3983, 10.1021/cr5003485, 2015.
Pasilis, S. P., Kertesz, V., and Van Berkel, G. J.: Unexpected analyte oxidation during desorption electrospray ionization-mass spectrometry, Anal. Chem., 80, 1208-1214, 10.1021/ac701791w, 2008.
Pourbafrani, M., Forgács, G., Horváth, I. S., Niklasson, C., and Taherzadeh, M. J.: Production of biofuels, limonene and pectin from citrus wastes, Bioresour. Technol., 101, 4246-4250, 10.1016/j.biortech.2010.01.077, 2010.
Ranzi, E., Cavallotti, C., Cuoci, A., Frassoldati, A., Pelucchi, M., and Faravelli, T.: New reaction classes in the kinetic modeling of low temperature oxidation of n-alkanes, Combust. Flame, 162, 1679-1691, 10.1016/j.combustflame.2014.11.030, 2015.
Ray, D. J. M., Redfearn, A., and Waddington, D. J.: Gas-phase oxidation of alkenes: decomposition of hydroxy-substituted peroxyl radicals, Journal of the Chemical Society, Perkin Transactions 2, 540-543, 10.1039/p29730000540, 1973.
Rissanen, M. P., Kurtén, T., Sipilä, M., Thornton, J. A., Kangasluoma, J., Sarnela, N., Junninen, H., Jørgensen, S., Schallhart, S., Kajos, M. K., Taipale, R., Springer, M., Mentel, T. F., Ruuskanen, T., Petäjä, T., Worsnop, D. R., Kjaergaard, H. G., and Ehn, M.: The Formation of Highly Oxidized Multifunctional Products in the Ozonolysis of Cyclohexene, Journal of the American Chemical Society, 136, 15596-15606, 10.1021/ja507146s, 2014.
Seinfeld, J. H., and Pandis, S. N.: Atmospheric Chemistry and Physics: From Air Pollution to Climate Change, 2nd ed., Wiley-Interscience, Hoboken, NJ, 1232 pp., ISBN: 978-1-118-94740-1, 2006.
Sleno, L.: The use of mass defect in modern mass spectrometry, Journal of Mass Spectrometry, 47, i-i, 10.1002/jms.2978, 2012.
Thion, S., Togbe, C., Serinyel, Z., Dayma, G., and Dagaut, P.: A chemical kinetic study of the oxidation of dibutyl-ether in a jet-stirred reactor, Combust. Flame, 185, 4-15, 10.1016/j.combustflame.2017.06.019, 2017.
Tu, P., Hall, W. A., and Johnston, M. V.: Characterization of Highly Oxidized Molecules in Fresh and Aged Biogenic Secondary Organic Aerosol, Analytical Chemistry, 88, 4495-4501, 10.1021/acs.analchem.6b00378, 2016.
Van Krevelen, D. W.: Graphical-statistical method for the study of structure and reaction processes of coal, Fuel, 29, 269-284, Corpus ID: 208705483,1950.
Walser, M. L., Desyaterik, Y., Laskin, J., Laskin, A., and Nizkorodov, S. A.: High-resolution mass spectrometric analysis of secondary organic aerosol produced by ozonation of limonene, Physical Chemistry Chemical Physics, 10, 1009-1022, 10.1039/B712620D, 2008.
Wang, Zhandong, Zhang, L., Moshammer, K., Shankar, V. S. B., Lucassen, A., Hemken, C., Taatjes, C. A., Leone, S. R., Kohse-Höinghaus, K., Hansen, N., Dagaut, P., and Sarathy, S. M.: Additional chain-branching pathways in the low-temperature oxidation of branched alkanes, Combustion and Flame, 164, 386-396, 10.1016/j.combustflame.2015.11.035, 2016.
Wang, X., Hayeck, N., Brüggemann, M., Yao, L., Chen, H., Zhang, C., Emmelin, C., Chen, J., George, C., and Wang, L.: Chemical Characteristics of Organic Aerosols in Shanghai: A Study by Ultrahigh-Performance Liquid Chromatography Coupled With Orbitrap Mass Spectrometry, Journal of Geophysical Research: Atmospheres, 122, 11,703-711,722, 10.1002/2017jd026930, 2017.
Wang, Z., Popolan-Vaida, D. M., Chen, B., Moshammer, K., Mohamed, S. Y., Wang, H., Sioud, S., Raji, M. A., Kohse-Höinghaus, K., Hansen, N., Dagaut, P., Leone, S. R., and Sarathy, S. M.: Unraveling the structure and chemical mechanisms

https://doi.org/10.5194/acp-2020-1070
Preprint. Discussion started: 8 December 2020

of highly oxygenated intermediates in oxidation of organic compounds, Proceedings of the National Academy of Sciences, 114, 13102-13107, 10.1073/pnas.1707564114, 2017.

Wang, Z., Herbinet, O., Hansen, N., and Battin-Leclerc, F.: Exploring hydroperoxides in combustion: History, recent advances and perspectives, Progress in Energy and Combustion Science, 73, 132-181, 10.1016/j.pecs.2019.02.003, 2019.

Wang, Z. D., Chen, B. J., Moshammer, K., Popolan-Vaida, D. M., Sioud, S., Shankar, V. S. B., Vuilleumier, D., Tao, T., Ruwe, L., Brauer, E., Hansen, N., Dagaut, P., Kohse-Hoinghaus, K., Raji, M. A., and Sarathy, S. M.: n-Heptane cool flame chemistry: Unraveling intermediate species measured in a stirred reactor and motored engine, Combust. Flame, 187, 199-216, 10.1016/j.combustflame.2017.09.003, 2018.

Warscheid, B., and Hoffmann, T.: Structural elucidation of monoterpene oxidation products by ion trap fragmentation using on-line atmospheric pressure chemical ionisation mass spectrometry in the negative ion mode, Rapid Communications in Mass Spectrometry, 15, 2259-2272, 10.1002/rcm.504, 2001.

Witkowski, B., and Gierczak, T.: Characterization of the limonene oxidation products with liquid chromatography coupled to the tandem mass spectrometry, Atmos. Environ., 154, 297-307, 10.1016/j.atmosenv.2017.02.005, 2017.

Wu, Z., Rodgers, R. P., and Marshall, A. G.: Two- and Three-Dimensional van Krevelen Diagrams: A Graphical Analysis Complementary to the Kendrick Mass Plot for Sorting Elemental Compositions of Complex Organic Mixtures Based on Ultrahigh-Resolution Broadband Fourier Transform Ion Cyclotron Resonance Mass Measurements, Analytical Chemistry, 76, 2511-2516, 10.1021/ac0355449, 2004.

Yanowitz, J., Ratcliff, M. A., McCormick, R. L., Taylor, J. D., and Murphy, M. J.: Compendium of Experimental Cetane Numbers, National Renewable Energy Lab. (NREL), Golden, CONREL/TP-5400-67585, 10.2172/1345058, 2017.

Zhang, H., Yee, L. D., Lee, B. H., Curtis, M. P., Worton, D. R., Isaacman-VanWertz, G., Offenberg, J. H., Lewandowski, M., Kleindienst, T. E., Beaver, M. R., Holder, A. L., Lonneman, W. A., Docherty, K. S., Jaoui, M., Pye, H. O. T., Hu, W., Day, D. A., Campuzano-Jost, P., Jimenez, J. L., Guo, H., Weber, R. J., de Gouw, J., Koss, A. R., Edgerton, E. S., Brune, W., Mohr, C., Lopez-Hilfiker, F. D., Lutz, A., Kreisberg, N. M., Spielman, S. R., Hering, S. V., Wilson, K. R., Thornton, J. A., and Goldstein, A. H.: Monoterpenes are the largest source of summertime organic aerosol in the southeastern United States, Proceedings of the National Academy of Sciences, 115, 2038-2043, 10.1073/pnas.1717513115, 2018.

Zhao, D. F., Kaminski, M., Schlag, P., Fuchs, H., Acir, I. H., Bohn, B., Häseler, R., Kiendler-Scharr, A., Rohrer, F., Tillmann, R., Wang, M. J., Wegener, R., Wildt, J., Wahner, A., and Mentel, T. F.: Secondary organic aerosol formation from hydroxyl radical oxidation and ozonolysis of monoterpenes, Atmos. Chem. Phys., 15, 991-1012, 10.5194/acp-15-991-2015, 2015.